Archiv für Elektrotechnik 77 (1994) 327–335 © Springer-Verlag 1994

Image theory for a point charge inside a layered dielectric sphere

J. C.-E. Sten, R. Ilmoniemi

Contents Following the approach of Neumann and Lindell [1] we derive an image line source that produces in a homogeneous medium the same electric field as a point charge inside a layered dielectric sphere. The image charge density function for the sphere with two interfaces is solved analytically, and approximations are derived in the case of a thin layer and a low-contrast layer. An image expression for the thin-layered sphere with three interfaces is developed. We suggest that point charge approximations of the image charge may be used to speed up computations of the electric potential on the scalp due to sources in the brain.

Elektrostatische Spiegelungstheorie für Punktladungen in einer geschichteten dielektrischen Kugel

Übersicht Basierend auf dem Ansatz von Neumann und Lindell [1] wird eine scheinbare Linienladung abgeleitet, die in einem homogenen Medium das gleiche elektrische Feld hervorruft wie eine Punktladung innerhalb einer geschichteten dielektrischen Kugel. Die Dichtefunktion der Bildladung für eine Kugel mit zwei Trennflächen wird analytisch bestimmt, und Näherungen für den Fall einer dünnen Schicht und einer nur kleinen Änderung der Permittivität werden abgeleitet. Eine Abbildung für eine Kugel aus dünnen Schichten mit drei Trennflächen wird entwickelt. Die Punktladungsnäherungen der Bildladungen können verwendet werden, um die Berechnung des elektrischen Potentials auf der Kopfhaut aufgrund von Qellen im Gehirn zu beschleunigen.

1 Introduction

The electric potential produced by a point charge outside a conducting sphere with zero net charge can be computed by replacing the sphere with a simple combination of image point charges. This well-known method, usually referred to as the Kelvin inversion [2], was recently generalized by Lindell [1] to the problem of a charge outside of a dielectric sphere. If a is the radius sphere and d the distance from the center of the sphere to the original charge, then the reflection image source consists of a charge at the Kelvin inversion point $d_K = a^2/d$ and a continuous line source between this point and the center of the sphere. It later turned out that a similar solution for the corresponding magnetostatic problem had been presented in an appendix of a book by Carl Neumann in 1883 [3], but has apparently not been applied since the original invention.

Following the rediscovery, a number of other electromagnetic problems involving spherical interfaces have been solved. In [4] it was demonstrated that a point charge q inside a dielectric sphere of radius a at a distance d from the center can be replaced by a line source extending from the external Kelvin image point $d_K = a^2/d$ to infinity when the internal potential is computed. For the external potential, the image lies between the original charge and the center of the sphere. In another paper [5] the layered sphere was analyzed in order to solve the reflection image of a point charge placed outside a dielectric multilayer sphere. A transmission-line analogy for spherical static fields was applied to find the reflected potential and the image for the two-interface sphere. The interaction of separate dielectric spheres in a homogeneous field was recently studied using the image method [6], and in the most recent contribution [7] the static image theory for the dielectric sphere was extended to the low-frequency domain.

In the present paper, a method is developed for deriving expressions for transmission image sources in the case of a point charge located inside a homogeneous sphere covered by concentric layers of different permittivity. When the expression for the transmitted potential is compared with the expression for the potential due to an image line charge, we obtain a set of equations for the image source. Analytical solutions are derived for the two-interface sphere with arbitrary radii, for the case of a thin layer, and for a thick layer of low permittivity contrast. The image for the three-interface sphere is solved in the thin-layer limit.

Images for dipolar sources can be derived by taking the gradient of the image for a point charge [4], or simply by superposition of images corresponding to a pair of charges of opposite sign. The present method can also be directly reformulated for the corresponding DC current problem, with general values for the layer conductivities of

Received 18 November 1993

J. Sten
Electromagnetics Laboratory
R. Ilmoniemi,
Low Temperature Laboratory, Helsinky University of Technology,
Fin-02150 Esbo, Finland

Correspondence to: J. Sten

This study was supported in part by the Academy of Finland. We thank Ismo V. Lindell, Olli V. Lounasmaa and Seppo Ahlfors for criticsm and comments.

the sphere and the surrounding material, just by replacing ε by conductivity σ and q by the source current amplitude. Similarly, the method can be applied to magnetostatics by replacing ε by permeability μ and q's by magnetic monopoles [8].

Our method may be useful, for instance, in the analysis of electric potentials that are produced by sources of current in the brain and measured from the human scalp. Normally, the head is modeled as a sphere consisting of 3 or 4 conducting layers [9–13], making the computations of the potential quite time-consuming. Since a point source in a multilayer sphere can be replaced by a line source in a homogeneous medium and this image source can be approximated by a small number of point sources, the possibility arises that the present method may lead to an algorithm allowing rapid computations of the electric field in electroencephalography.

2 Theory

Consider an electric point charge q located inside a sphere composed of $N-1$ concentric dielectrically homogeneous regions (Fig. 1). The origin of coordinates is at the center of the sphere; q is assumed to be inside the innermost region on the z-axis at $z=d$. The radii of the spherical interfaces are labeled $a_1 > a_2 > \ldots > a_{N-1}$ and the permittivities of the regions $\varepsilon_2, \ldots, \varepsilon_N$ respectively, with ε_1 being the permittivity of the spurrounding medium. Our task is to compute the electric potential ϕ, which is related to the charge by

$$\nabla \cdot (\varepsilon \mathbf{E}) = q\delta(\mathbf{r} - d\mathbf{u}_z), \tag{1}$$

where the electric field $\mathbf{E} = -\nabla\phi$; in homogeneous source-free regions (1) reduces to the Laplace equation $\nabla^2\phi = 0$.

Our problem is rotationally symmetric with respect to the z-axis, which allows the potential to be written in terms of Legendre polynomials [13, pp. 204–205], viz.,

$$\phi(r, \theta) = \sum_{n=0}^{\infty} [A_n r^n + B_n r^{-(n+1)}] P_n(\cos\theta), \tag{2}$$

where r and θ are the spherical coordinates of the field point and $P_n(x)$ denotes the n th-order Legendre polynomial of the first kind. The potential in each region is expressed as follows:

$$\phi_1(r, \theta) = \sum_{n=0}^{\infty} B_n^1 r^{-(n+1)} P_n(\cos\theta) \qquad r \geqq a_1 \tag{3}$$

$$\phi_2(r, \theta) = \sum_{n=0}^{\infty} [A_n^2 r^n + B_n^2 r^{-(n+1)}] P_n(\cos\theta) \qquad a_1 \geqq r \geqq a_2 \tag{4}$$

$$\phi_N(r, \theta) = \sum_{n=0}^{\infty} [A_n^N r^n + B_n^N r^{-(n+1)}] P_n(\cos\theta) \qquad a_{N-1} \geqq r \geqq d \tag{5}$$

$$\phi_{N+1}(r, \theta) = \sum_{n=0}^{\infty} A_n^{N+1} P_n(\cos\theta) \qquad r < d. \tag{6}$$

Each term in these expressions represents a 'mode' of potential: the ones with A-coefficients grow as r^n, while those with B-coefficients diverge at the origin. Since ϕ is finite everywhere, $B_n^{N+1} \equiv 0$ and $A_n^1 \equiv 0$.

The tangential component of E and the normal component of the displacement vector $\mathbf{D} = \varepsilon\mathbf{E}$ are required to be continuous, implying that ϕ and $\varepsilon\partial\phi/\partial r$ must be continuous et each spherical boundary. This allows the unknown coefficients A_n^k and B_n^k to be determined. For example, at $r = a_2$, we have

$$\phi_2(a_2, \theta) = \phi_3(a_2, \theta), \tag{7}$$

$$\varepsilon_2 \frac{\partial\phi_2}{\partial r}(a_2, \theta) = \varepsilon_3 \frac{\partial\phi_3}{\partial r}(a_2, \theta). \tag{8}$$

Because of orthogonality of the Legendre polynomials, the modes with different n are uncoupled. Thus, from Eqs. (7) and (8),

$$A_n^2 a_2^n + B_n^2 a_2^{-(n+1)} = A_n^3 a_2^n + B_n^3 a_2^{-(n+1)}, \tag{9}$$

$$\varepsilon_2\left(nA_n^2 a_2^n - (n+1)\, B_n^2 a_2^{-(n+1)}\right) = \varepsilon_3\left(nA_n^3 a_2^n - (n+1)\, B_n^3 a_2^{-(n+1)}\right). \tag{10}$$

These equations can be written [5] as

$$B_n^2 = R_n^{23} A_n^2 a_2^{2n+1} + T_n^{32} B_n^3 \tag{11}$$

$$A_n^3 = T_n^{23} A_n^2 + R_n^{32} a_2^{-(2n+1)}\, B_n^3, \tag{12}$$

where we have introduced the dimensionless reflection and transmission coefficients for the static fields at interface a_2:

$$R_n^{23} = \frac{n(\varepsilon_2 - \varepsilon_3)}{\varepsilon_3 n + \varepsilon_2(n+1)}, \qquad R_n^{32} = \frac{(n+1)\,(\varepsilon_3 - \varepsilon_2)}{\varepsilon_3 n + \varepsilon_2(n+1)}, \tag{13}$$

$$T_n^{23} = \frac{\varepsilon_2(2n+1)}{\varepsilon_3 n + \varepsilon_2(n+1)}, \qquad T_n^{32} = \frac{\varepsilon_3(2n+1)}{\varepsilon_3 n + \varepsilon_2(n+1)}. \tag{14}$$

Coefficients relating the potential across the other interfaces can be obtained similarly. For example, from (3) and (4),

$$B_n^1 = T_n^{21} B_n^2 = \frac{\varepsilon_2(2n+1)}{\varepsilon_3 n + \varepsilon_1(n+1)}\, B_n^2,$$

$$A_n^2 = R_n^{21} \frac{B_n^2}{a_1^{2n+1}} = \frac{(n+1)\,(\varepsilon_2 - \varepsilon_1)}{\varepsilon_2 n + \varepsilon_1(n+1)} \frac{B_n^2}{a_1^{2n+1}}. \tag{15}$$

To proceed, we must now derive the coefficients B_n^N, $n = 1, 2, \ldots$ All others can then be found by applying

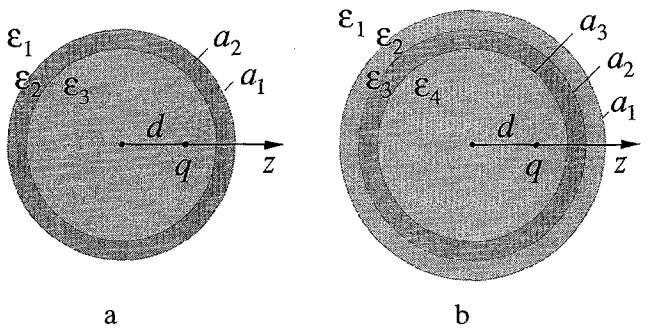

Fig. 1a, b. Geometry of a the two-interface problem and b the three-interface problem. An electric point charge lies inside a dielectric sphere covered by concentric spherical layers of different permittivity. The origin of coordinates is at the center of the sphere

transmission and reflection formulas such as Eqs. (11) and (12).

If the effects of boundaries were ignored, the potential due to q would be inversely proportional to the distance from the charge. We expand this incident potential into an infinite sum of Legendre polynomials [14]:

$$\frac{q}{4\pi\varepsilon_N |\mathbf{r}-\mathbf{u}_z d|} = \frac{q}{4\pi\varepsilon_N r} \sum_{n=0}^{\infty} \left(\frac{d}{r}\right)^n P_n(\cos\theta), \qquad r > d, \quad (16)$$

where $|\mathbf{r}-\mathbf{u}_z d| = \sqrt{r^2 + d^2 - 2rd\cos\theta}$ is the distance from the charge to $\mathbf{r}$. Comparison with expression (5) gives $B_n^N = qd^n/4\pi\varepsilon_N$. To solve for the transmitted field we must relate B_n^1 to B_n^N by using the set of equations obtained through the boundary conditions. Instead of being satisfied with this, we determine an equivalent line source such that all coefficients in its Legendre expansion outside the sphere are the same at those of the original source.

2.1
Transmission image problem

The potential ϕ_1 outside the sphere can be interpreted as arising from an image line with charge density $\varrho_i(z)$, extending from the origin to $z = d$. As shown in [4],

$$\phi_i(r,\theta) = \frac{1}{4\pi\varepsilon_1} \int_0^d \frac{\varrho_i(z')\,dz'}{\sqrt{r^2 + z'^2 - 2rz'\cos\theta}}$$

$$= \frac{1}{4\pi\varepsilon_1 r} \sum_{n=0}^{\infty} P_n(\cos\theta) \int_0^d \varrho_i(z') \left(\frac{z'}{r}\right)^n dz'. \qquad (17)$$

By comparing Eq. (17) with expression (3) and by applying the orthogonality of Legendre polynomials, we are led to a set of integral equations for $\varrho_i(z)$, viz.

$$B_n^1 = \frac{1}{4\pi\varepsilon_1} \int_0^d \varrho_i(z')\, z'^n\, dz', \qquad n = 1, 2, \ldots. \qquad (18)$$

This is a modification of the Mellin integral transform, the integration interval being finite [5]. Once $\varrho_i(z)$ has been found, the potential can be calculated by the integration expressed in (17).

2.2
Sphere with two interfaces

Let us apply the method outlined above to a sphere with two interfaces, $N = 3$ (Fig. 1a). Because $A_n^1 = 0$, the expression for the coefficients B_n^1 can be obtained in a straightforward manner from (11) and (15):

$$B_n^1 = \frac{T_n^{21} T_n^{32} B_n^3}{1 - R_n^{23} R_n^{21} (a_2/a_1)^{2n+1}}, \qquad (19)$$

with

$$B_n^3 = \frac{q}{4\pi\varepsilon_3} d^n. \qquad (20)$$

A substitution of the expressions for the reflection and transmission coefficients into Eq. (19) results in a rather complicated expression, for which the finite Mellin transformation is not available. Let us, therefore, express Eq. (19) by a sum of a geometrical series, as was done in [5]:

$$B_n^1 = T_n^{21} T_n^{32} B_n^3 \sum_{k=0}^{\infty} [R_n^{23} R_n^{21} (a_2/a_1)^{2n+1}]^k = \sum_{k=0}^{\infty} B_{n_k}^1. \qquad (21)$$

This is allowed because $a_2 < a_1$ and $|R_n^{23} R_n^{21}| \leqq 1$ for all values $n = 0, 1, 2, \ldots$ and for arbitrary permittivities $\varepsilon_1, \varepsilon_2, \varepsilon_3$. A general term in (21) can be expressed as

$$B_{n_k}^1 = \frac{\varepsilon_2\varepsilon_3 (2n+1)^2 (n^2+n)^k (\varepsilon_2-\varepsilon_1)^k (\varepsilon_2-\varepsilon_3)^k (a_2/a_1)^k}{\left[(\varepsilon_1+\varepsilon_2)(\varepsilon_2+\varepsilon_3)\left(n+\frac{\varepsilon_1}{\varepsilon_2+\varepsilon_1}\right)\left(n+\frac{\varepsilon_2}{\varepsilon_2+\varepsilon_3}\right)\right]^{k+1}}$$
$$\times \left[\left(\frac{a_2}{a_1}\right)^{2k}\right]^n B_n^3. \qquad (22)$$

Before deriving the exact image expression, let us illustrate the method by dividing the first term in Eq. (21) into partial fractions:

$$B_{n_0}^1 = T_n^{21} T_n^{32} B_n^3$$
$$= \frac{\varepsilon_2\varepsilon_3 (2n+1)^2}{(\varepsilon_2+\varepsilon_3)(\varepsilon_1+\varepsilon_2)\left(n+\frac{\varepsilon_1}{\varepsilon_1+\varepsilon_2}\right)\left(n+\frac{\varepsilon_2}{\varepsilon_2+\varepsilon_3}\right)} B_n^3$$
$$= \frac{\varepsilon_2 q d^n}{4\pi(\varepsilon_1\varepsilon_3 - \varepsilon_2^2)} \left[\frac{4(\varepsilon_1\varepsilon_3 - \varepsilon_2^2)}{(\varepsilon_1+\varepsilon_2)(\varepsilon_2+\varepsilon_3)}\right.$$
$$\left. + \left(\frac{\varepsilon_3-\varepsilon_2}{\varepsilon_3+\varepsilon_2}\right)^2 \frac{1}{\left(n+\frac{\varepsilon_2}{\varepsilon_2+\varepsilon_3}\right)} - \left(\frac{\varepsilon_1-\varepsilon_2}{\varepsilon_1+\varepsilon_2}\right)^2 \frac{1}{\left(n+\frac{\varepsilon_1}{\varepsilon_1+\varepsilon_2}\right)}\right] \qquad (23)$$

Noticing that the first term in the square-bracketed expression is independent of n and the last two the form $1/(n+\alpha)$, we can apply Eq. (18) using the following identities:

$$\int_0^1 \delta_-(x-x_0)\, x^n\, dx = x_o^n, \qquad \int_0^{x_o} x_o^{-\alpha} x^{\alpha-1} x^n\, dx = \frac{x_o^n}{n+\alpha};$$
$$0 < x_o \leqq 1. \qquad (24)$$

Here, we must use $\delta_-(x) = \lim_{\Delta\to 0}\delta(x-\Delta)$, with $\Delta > 0$. This definition is needed only when $x_0 = 1$. Substituting $x = z'/d$ in the above transformations, the image function $\varrho_{i_0}(z)$, corresponding to Eq. (23), can be found:

$$\varrho_{i_0}(z) = \frac{4q\varepsilon_1\varepsilon_2}{(\varepsilon_1+\varepsilon_2)(\varepsilon_2+\varepsilon_3)}\delta(z-d),$$
$$+ \frac{q\varepsilon_1\varepsilon_2}{d(\varepsilon_1\varepsilon_3-\varepsilon_2^2)}\left[\left(\frac{\varepsilon_3-\varepsilon_2}{\varepsilon_3+\varepsilon_2}\right)^2 \left(\frac{z}{d}\right)^{-\varepsilon_3/(\varepsilon_2+\varepsilon_3)}\right.$$
$$\left. - \left(\frac{\varepsilon_2-\varepsilon_1}{\varepsilon_2+\varepsilon_1}\right)^2 \left(\frac{z}{d}\right)^{-\varepsilon_2/(\varepsilon_1+\varepsilon_2)}\right] \prod(0, z, d), \qquad (25)$$

where $\prod(a, z, b)$ denotes the pulse function, i.e., the product of two unit step functions

$$\prod(a, z, b) = U(z-a)\, U(b-z) = 1 \quad \text{for} \quad a < z < b$$
$$= 0 \quad \text{elsewhere.} \tag{26}$$

The parameters of this lowest-order approximation of the image source do not depend on the radii of the interfaces. It is seen from Eq. (19) that this is accurate in the limit of small a_2/a_1. The result can be checked by setting either $\varepsilon_1 = \varepsilon_2$ or $\varepsilon_2 = \varepsilon_3$; Eq. (25) then reproduces the image source for a homogeneous sphere, derived in [4]:

$$\varrho_i(z) = \frac{2}{\varepsilon_r + 1}\, q\delta(z-d) + \frac{\varepsilon_r - 1}{(\varepsilon_r+1)^2}\,\frac{q}{d}\left(\frac{z}{d}\right)^{-\varepsilon_r/(\varepsilon_r+1)} \prod(0, z, d), \tag{27}$$

where $\varepsilon_r = \varepsilon_3/\varepsilon_1$ is the relative permittivity. The total charge of (27) is q, as can be verified by integration. In contradistinction of Eq. (25) does not give q, because it is only a portion of the equivalent source. Also, when all permittivities are the same, i.e., when the sphere vanishes, the continuous part of $\varrho_i(z)$ in (25) vanishes, leaving the original point charge $q\delta(z-d)$. In the limit $\varepsilon_3 \to \infty$, which corresponds to a perfectly conducting sphere, the amplitude of the delta peak vanishes, whereas the first part of the continuous image function approaches a delta function at the origin. Thus, the transmitted potential appears to originate at the center of the sphere with no dependence on the position of the original charge. It can also be noted, as a brief check, that because the original point charge $q\delta(z-d)$ inside a homogeneous sphere can be replaced by an image charge density function with a delta function part, viz., $2\varepsilon_1 q\delta(z-d)/(\varepsilon_2+\varepsilon_1)$, the corresponding image charge density function with respect to the outermost interface a_1 is $4\varepsilon_1\varepsilon_2 q\delta(z-d)/(\varepsilon_3+\varepsilon_2)\,(\varepsilon_1+\varepsilon_2)$, which agrees with the results in Eq. (25).

2.2.1 Exact solution

In order to solve the complete image charge expression for the sphere with two interfaces, we must consider Eq. (22) in the form

$$B^1_{n_k} = \frac{P(n)}{Q(n)}\left[\left(\frac{a_2}{a_1}\right)^{2k}\right]^n B^3_n, \tag{28}$$

where both $P(n)$ and $Q(n)$ are polynomials of degree $2k+2$. Thus, we can directly accomplish the division as

$$\frac{P(n)}{Q(n)} = \frac{4\varepsilon_3\varepsilon_2(\varepsilon_2-\varepsilon_1)^k(\varepsilon_2-\varepsilon_3)^k}{(\varepsilon_1+\varepsilon_2)^{k+1}(\varepsilon_2+\varepsilon_3)^{k+1}}\left(\frac{a_2}{a_1}\right)^k + \frac{X(n)}{Q(n)}, \tag{29}$$

where the remainder polymial $X(n)$ is of degree $2k+1$. Each $k = 0, 1, 2, \ldots$ will produce a delta function of different amplitude and location according to Eq. (24). Furthermore, $X(n)$ can be decomposed into partial fractions of two repeated linear factors as follows:

$$\frac{X(n)}{Q(n)} = \frac{\varepsilon_2\varepsilon_3(\varepsilon_2-\varepsilon_1)^k(\varepsilon_2-\varepsilon_3)^k\,(a_2/a_1)^k}{(\varepsilon_1+\varepsilon_2)^{k+1}(\varepsilon_2+\varepsilon_3)^{k+1}} \times \sum_{i=1}^{k+1}\left[\frac{A_{k,i}}{\left(n+\frac{\varepsilon_1}{\varepsilon_1+\varepsilon_2}\right)^i} + \frac{B_{k,i}}{\left(n+\frac{\varepsilon_2}{\varepsilon_2+\varepsilon_3}\right)^i}\right]. \tag{30}$$

Coefficients $A_{k,i}$ and $B_{k,i}$ can be evaluated from the following recursion formulas involving differentiations

$$A_{k,i} = \frac{1}{(k+1-i)!}\,\frac{d^{k+1-i}}{dn^{k+1-i}}\left[\frac{(2n+1)^2\,(n^2+n)^k}{\left(n+\frac{\varepsilon_2}{\varepsilon_2+\varepsilon_3}\right)^{k+1}}\right]_{n=-\varepsilon_1/(\varepsilon_1+\varepsilon_2)} \tag{31}$$

$$B_{k,i} = \frac{1}{(k+1-i)!}\,\frac{d^{k+1-i}}{dn^{k+1-i}}\left[\frac{(2n+1)^2\,(n^2+n)^k}{\left(n+\frac{\varepsilon_1}{\varepsilon_1+\varepsilon_2}\right)^{k+1}}\right]_{n=-\varepsilon_2/(\varepsilon_2+\varepsilon_3)}, \tag{32}$$

where $i = 1, 2, \ldots, k+1$. Note that in the special case of $\varepsilon_2 = \sqrt{\varepsilon_1\varepsilon_3}$, both $A_{k,i}$ and $B_{k,i}$ are singular, implying that the fractional expansion must involve only one repeated factor.

Applying the idently [15]

$$\frac{1}{(p-1)!}\int_0^{x_o}\left[\ln\left(\frac{x_o}{x}\right)\right]^{p-1}\left(\frac{x}{x_o}\right)^{\alpha-1} x^n\,dx = \frac{x_o^{n+1}}{(n+\alpha)^p}$$
$$0 < x_o < 1, \tag{33}$$

the complete image line charge function for the sphere with two interfaces becomes

$$\varrho_i(z) = \frac{\varepsilon_1\varepsilon_2 q}{(\varepsilon_1+\varepsilon_2)(\varepsilon_2+\varepsilon_3)}\sum_{k=0}^{\infty}\left[\frac{(\varepsilon_1-\varepsilon_1)(\varepsilon_2-\varepsilon_3)}{(\varepsilon_1+\varepsilon_2)(\varepsilon_2+\varepsilon_3)}\right]^k \times\left\{4\left(\frac{a_2}{a_1}\right)^k\delta\left(z-d\left(\frac{a_2}{a_1}\right)^{2k}\right) + \sum_{i=1}^{k+1}\left(\frac{a_{12}}{a_2}\right)^k\frac{\left[\ln\left(\left(\frac{a_2}{a_1}\right)^{2k}\frac{d}{z}\right)\right]^{i-1}}{d(i-1)!} \times\left[A_{k,i}\left(\left(\frac{a_2}{a_1}\right)^{2k}\frac{d}{z}\right)^{\varepsilon_2/\varepsilon_1+\varepsilon_2} + B_{k,i}\left(\left(\frac{a_2}{a_1}\right)^{2k}\frac{d}{z}\right)^{\varepsilon_3/\varepsilon_2+\varepsilon_3}\right] \times\prod\left[0, \frac{z}{d}, \left(\frac{a_2}{a_1}\right)^{2k}\right]\right\}. \tag{34}$$

The first part of $\varrho_i(z)$ consists of delta functions whose amplitudes decrease with increasing k while their locations approach the center of the sphere. The second part is a series of continuous functions extending from the center to the location of the k th delta function. The adequate number of terms in the series depends on the ratio of the radii so that when the layer is very thick ($a_2/a_1 \ll 1$), only a few terms are needed. The same applies when the permittivities of adjacent regions are close to each other. On the other hand, for thin layers ($a_2 \approx a_1$), the series converges slowly, and therefore, the

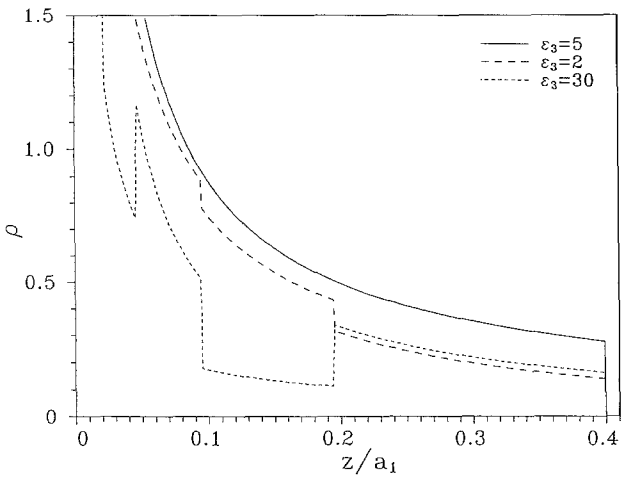

Fig. 2. Normalized image line charge density function $\varrho_i(z)$ corresponding to a two-interface sphere for varying ε_3. The normalized permittivities are $\varepsilon_1 = 1$, $\varepsilon_2 = 5$, and $\varepsilon_2 = 0.7a_1$. (Delta functions are not shows.) The original charge lies at $d = 0.4a_1$. In the case $\varepsilon_3 = 5$ the curve is smooth and resembles the image for the homogeneous sphere of $\varepsilon_r = 5$

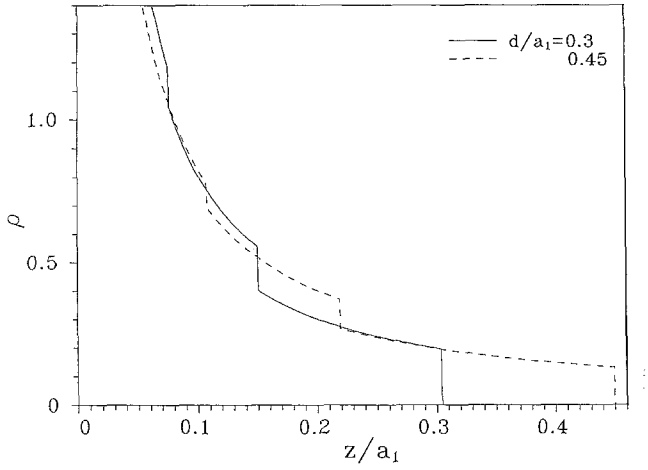

Fig. 3. Normalized image line charge density function $\varrho_i(z)$ corresponding to a two-interface sphere with the normalized permittivities $\varepsilon_1 = 1$, $\varepsilon_2 = 10$, $\varepsilon_3 = 5$ and $\varepsilon_2 = 0.7a_1$. The location of the original sources are $d = 0.3a_1$ and $d = 0.45a_1$

image must be approximated, as shown in the following section. Some examples of the continuous part of the image line charge function are depicted in Figs. 2–4 when some of the parameters are varied. Note that although the image is singular at the origin its integral (33) is finite valued.

2.2.2 Special cases

Approximate expresssions can be obtained for certain special cases such as thin layers or for the case when the permitivity ratio across an interface is nearly unity (low constrast). A possible application for the thin-layer approximation is offered by the human head in the analysis of electroencephalography, where the layers in question are the skull and the scalp.

Thin layer: When the layer is thin, Eq. (19) can be approximated as

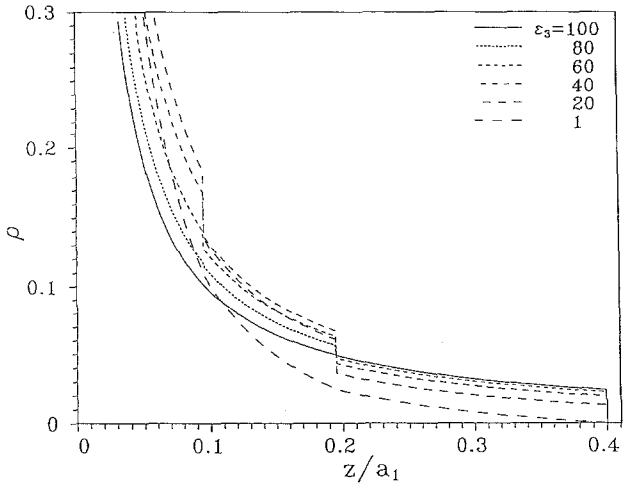

Fig. 4. Normalized image line charge density function $\varrho_i(z)$ with $\varepsilon_1 = 1$, $\varepsilon_2 = 100$, and $a_2 = 0.7a_1$, $d = 0.4a_1$. The curves are calculated for varying ε_3

$$B_n^1 \approx \frac{T_n^{21} T_n^{32} B_n^3}{1 - R_n^{23} R_n^{21} + a_r (2n+1)\, R_n^{23} R_n^{21}}, \tag{35}$$

where $a_r = a_2/a_1 \ll 1$. Letting $a_r \to 0$, i.e., approaching the limit of no layer,

$$B_n^1 \to \frac{T_n^{21} T_n^{32} B_n^3}{1 - R_n^{23} R_n^{21}} = \frac{(2n+1)\,\varepsilon_3}{n(\varepsilon_1 + \varepsilon_3) + \varepsilon_1} \frac{qd^n}{4\pi\varepsilon_3}, \tag{36}$$

from which the dependence of ε_2 has vanished. In fact, this expression contains the transmission coefficient T_n^{31} for a homogeneous sphere of relative permittivity $\varepsilon_3/\varepsilon_1$. This agress with the result for $\varepsilon_3 = \varepsilon_2$, whence the reflection and transmission coefficients at the interface a_2 become $R_n^{23} = 0$ and $T_n^{32} = 1$, respectively. The corresponding transmission image source is known to be of the form (27).

Approximating Eq. (35) further, we obtain

$$B_n^1 \approx \frac{T_n^{21} T_n^{32}}{(1 - R_n^{23} R_n^{21})} \left[1 - \frac{R_n^{23} R_n^{21}}{(1 - R_n^{23} R_n^{21})} (2n+1)\, a_r \right] B_n^3$$

$$= (T_n^{31} - a_r \xi)\, B_n^3. \tag{37}$$

It must be pointed out that this approximation will limit not only the thickness but also the value of ε_2. In fact, for the number of terms, n to be sufficient, the condition

$$a_r \ll \frac{\varepsilon_2 [n(\varepsilon_1 + \varepsilon_3) + \varepsilon_1}{n(n+1)\,(\varepsilon_2 - \varepsilon_3)\,(\varepsilon_2 - \varepsilon_1)}, \tag{38}$$

must hold. The conditions $a_r \to 0$, $\varepsilon_2 \to \infty$,and $a_r \varepsilon_2$ constant, characterize a dielectric sheet.

In expression (37), T_n^{31} is the transmission coefficient for a sphere, whereas ξ represents the perturbation due to

the layer. Writing ξ in partial fractions,

$$\xi = \frac{\varepsilon_3(\varepsilon_2-\varepsilon_3)\,(\varepsilon_2-\varepsilon_1)}{\varepsilon_2(\varepsilon_1+\varepsilon_3)^2} \times \left[2n + \frac{3\varepsilon_3-\varepsilon_1}{\varepsilon_1+\varepsilon_3} + \frac{1-\dfrac{6\varepsilon_1\varepsilon_3}{(\varepsilon_1+\varepsilon_3)^2}}{\left(n+\dfrac{\varepsilon_1}{\varepsilon_1+\varepsilon_2}\right)} + \frac{\dfrac{\varepsilon_1\varepsilon_3(\varepsilon_1-\varepsilon_3)}{(\varepsilon_1+\varepsilon_3)^3}}{\left(n+\dfrac{\varepsilon_1}{\varepsilon_1+\varepsilon_3}\right)^2} \right], \tag{39}$$

we are able to apply the finite Mellin transform (18) using Eqs. (24) and (33) plus the following transformation identity

$$\int_0^1 x^n \delta'_-(x-1)\,\mathrm{d}x = -nx^{n-1}\Big|_{x=1} = -n, \tag{40}$$

which follows from the definition of the derivatives of the delta function. Note that (40) holds only for the δ_- function because of the upper limit of the integral. Hence, the image charge density function can be written as

$$\begin{aligned} \varrho_i(z) = {} & \frac{2\varepsilon_1}{\varepsilon_3+\varepsilon_1}\, q\delta(z-d) \\ & + \frac{\varepsilon_1(\varepsilon_3-\varepsilon_1)}{(\varepsilon_3+\varepsilon_1)^2}\,\frac{q}{d}\left(\frac{z}{d}\right)^{-\varepsilon_3/(\varepsilon_3+\varepsilon_1)} \prod(0,z,d) \\ & - a_r q\,\frac{\varepsilon_1}{\varepsilon_3}\left[\xi_1\delta'(d-z) + \xi_2\delta(z-d) \right. \\ & \left. + \frac{1}{d}\left(\frac{z}{d}\right)^{-\varepsilon_3/(\varepsilon_3+\varepsilon_1)} \left(\xi_3 + \xi_4 \ln\left(\frac{d}{z}\right)\right) \prod(0,z,d) \right], \end{aligned} \tag{41}$$

where

$$\xi_1 = 2\,\frac{\varepsilon_3(\varepsilon_2-\varepsilon_3)\,(\varepsilon_2-\varepsilon_1)}{\varepsilon_2(\varepsilon_1+\varepsilon_3)^2} \tag{42}$$

$$\xi_2 = \frac{\varepsilon_3(\varepsilon_2-\varepsilon_3)\,(\varepsilon_2-\varepsilon_1)\,(3\varepsilon_3-\varepsilon_1)}{\varepsilon_2(\varepsilon_1+\varepsilon_3)^3} \tag{43}$$

$$\xi_3 = \frac{\varepsilon_3(\varepsilon_2-\varepsilon_3)\,(\varepsilon_2-\varepsilon_1)\,((\varepsilon_3+\varepsilon_1)^2-6\varepsilon_1\varepsilon_3)}{\varepsilon_2(\varepsilon_1+\varepsilon_3)^4} \tag{44}$$

$$\xi_4 = \frac{\varepsilon_1\varepsilon_3^2(\varepsilon_2-\varepsilon_3)\,(\varepsilon_2-\varepsilon_1)\,(\varepsilon_1-\varepsilon_3)}{\varepsilon_2(\varepsilon_1+\varepsilon_3)^5}. \tag{45}$$

In addition to the usually appearing combination of point line sources, expression (41) also contains a dipolar (δ') term. This can be understood to result from two image line charges of opposite polarity which do not totally overlap. From the above coefficients it can easily be established that if the permittivities of adjacent regions are the same, the perturbational part of the image charge function vanishes.

Low contrast: When the permittivity ratio between the layer and the homogeneous sphere is close to unity, Eq. (19) can be simplified. Defining the dimensionless number Δ_ε by

$$\Delta_\varepsilon = \varepsilon_3/\varepsilon_2 - 1, \tag{46}$$

the reflection and transmission coefficients corresponding to the interface $r = a_2$ can be written as

$$R_n^{23} = \frac{-n\Delta_\varepsilon}{(2n+1)+\Delta_\varepsilon n}, \qquad T_n^{32} = \frac{(\Delta_\varepsilon+1)\,(2n+1)}{(2n+1)+\Delta_\varepsilon n}. \tag{47}$$

Assuming $\Delta_\varepsilon \ll 1$, expression (19) can be approximated:

$$B_n^1 \approx (T_n^{21} - \Delta_\varepsilon\xi)\,\frac{qd^n}{4\pi\varepsilon_2}, \tag{48}$$

with the perturbational term

$$\zeta = \frac{n^2\varepsilon_2^2 + (n^2+n)\,[\varepsilon_1\varepsilon_2 + (\varepsilon_2^2-\varepsilon_1\varepsilon_2)\,(a_2/a_1)^{2n+1}]}{(\varepsilon_2 n + \varepsilon_1(n+1))^2}. \tag{49}$$

When $\Delta_\varepsilon \to 0$, the contribution of the layer disappears in (48), leaving the term with the transmission coefficient T_n^{21}. The image source corresponding to this term is obviously of the form (27).

Writing (49) in partial fractions,

$$\begin{aligned} \zeta = {} & \frac{\varepsilon_2}{\varepsilon_1+\varepsilon_2} - \frac{\varepsilon_1\varepsilon_2}{(\varepsilon_1+\varepsilon_2)\,(n\varepsilon_2+\varepsilon_1 n+1))} \\ & + \left(\frac{a_2}{a_1}\right)^{2n+1} \left[\frac{\varepsilon_2(\varepsilon_2-\varepsilon_1)}{(\varepsilon_1+\varepsilon_2^2)} + \frac{\varepsilon_2(\varepsilon_2-\varepsilon_1)^2}{(\varepsilon_1+\varepsilon_2)^2\,(n\varepsilon_2+\varepsilon_1(n+1))} \right. \\ & \left. + \frac{\varepsilon_1\varepsilon_2^2(\varepsilon_1-\varepsilon_2)}{(\varepsilon_1+\varepsilon_2)^2\,(n\varepsilon_2+\varepsilon_1(n+1))^2} \right], \end{aligned} \tag{50}$$

and applying the finite Mellin transformation with Eqs. (24) and (33), the complete image source corresponding to Eq. (48) becomes

$$\begin{aligned} \varrho_i(z) = {} & \frac{2\varepsilon_1}{\varepsilon_2+\varepsilon_1}\, q\delta(z-d) \\ & + \frac{\varepsilon_1\varepsilon_2-\varepsilon_1^2}{(\varepsilon_2+\varepsilon_1)^2}\,\frac{q}{d}\left(\frac{z}{d}\right)^{-\varepsilon_2/(\varepsilon_2+\varepsilon_1)} \prod(0,z,d) \\ & - \Delta_\varepsilon q \left\{ \zeta_1\delta(z-d) + \zeta_2\delta\left[z - d\left(\frac{a_2}{a_1}\right)^2\right] \right. \\ & + \frac{\zeta_3}{d}\left(\frac{z}{d}\right)^{-\varepsilon_2/(\varepsilon_2+\varepsilon_1)} \prod(0,z,d) + \left[\frac{\zeta_4}{d}\left(\frac{z}{d}\right)^{-\varepsilon_2/(\varepsilon_1+\varepsilon_2)} \right. \\ & \left. \left. + \frac{\zeta_5}{d}\ln\left(\frac{da_2^1}{za_2^2}\right)\left(\frac{za_1^2}{da_2^2}\right)^{-\varepsilon_2/(\varepsilon_1+\varepsilon_2)} \right] \prod\left[0,z,d\left(\frac{a_2}{a_1}\right)^2\right] \right\}, \end{aligned} \tag{51}$$

where

$$\zeta_1 = \frac{\varepsilon_1}{\varepsilon_1+\varepsilon_2} \tag{52}$$

$$\zeta_2 = \frac{\varepsilon_1(\varepsilon_2-\varepsilon_1)}{(\varepsilon_1+\varepsilon_2)^2}\,\frac{a_2}{a_1} \tag{53}$$

$$\zeta_3 = \frac{\varepsilon_1^2}{(\varepsilon_1+\varepsilon_2)^2} \tag{54}$$

$$\zeta_4 = \frac{\varepsilon_1(\varepsilon_2-\varepsilon_1)^2}{(\varepsilon_1+\varepsilon_2)^3}\left(\frac{a_2}{a_1}\right)^{(\varepsilon_2-\varepsilon_1)/(\varepsilon_2+\varepsilon_1)} \tag{55}$$

$$\zeta_5 = \frac{\varepsilon_1^2\varepsilon_2(\varepsilon_1-\varepsilon_2)}{(\varepsilon_1+\varepsilon_2)^4}\left(\frac{a_2}{a_1}\right)^{(\varepsilon_2-\varepsilon_1)/(\varepsilon_2+\varepsilon_1)}. \tag{56}$$

The first part of the image function is obviously due to the homogeneous sphere as if there were no layer present, whereas the rest of the terms are caused by the low-contrast layer. This result can also obtained using approximation (46) directly with (34).

2.3 Approximation for a three-interface sphere

For the sphere that has more than two interfaces, the routine of solving for B_n^1 becomes more involved and laborious. For example, considering a sphere with three interfaces of radii $a_1 \geqq a_2 \geqq a_3$ ($N=4$; Fig. 1b), we obtain

$$B_n^1 = T_n^{21}T_n^{32}T_n^{43}B_n^4\left\{1 - R_n^{34}R_n^{32}\left(\frac{a_3}{a_2}\right)^{2n+1} - R_n^{23}R_n^{21}\left(\frac{a_2}{a_1}\right)^{2n+1} + R_n^{23}R_n^{21}R_n^{34}R_n^{32} - R_n^{34}R_n^{21}T_n^{32}T_n^{23}\right]\left(\frac{a_3}{a_1}\right)^{2n+1}\Bigg\}^{-1}. \tag{57}$$

This is seen to agree with expression (19) when $R_n^{34}=0$ and $T_n^{43}=1$, as well as when two interfaces coincide. Due to the complexity, there is no advantage in writing this expression as a sum as was done in the previous case. There are, however, many possibilities to approximate, e.g., by assuming an equal ratio of the radii of adjacent interfaces in terms of the parameter a_r:

$$a_3/a_2 = a_2/a_1 = 1 - a_r. \tag{58}$$

When $a_r \ll 1$, i.e., with thin layers, $a_3/a_1 \ll 1-2a_r$, and the approximation for Eq. (57) reads

$$B_n^1 \approx \frac{T_n^{21}T_n^{32}T_n^{43}B_n^4}{1 - R_n^{34}R_n^{32} - R_n^{23}R_n^{21} + R_n^{23}R_n^{21}R_n^{34}R_n^{32} - R_n^{34}R_n^{21}T_n^{32}T_n^{23}} \times\left\{1 - a_r(2n+1) \times\frac{R_n^{34}R_n^{32} + R_n^{23}R_n^{21} - R_n^{23}R_n^{21}R_n^{34}R_n^{32} + R_n^{34}R_n^{21}T_n^{32}T_n^{23}}{1 - R_n^{34}R_n^{32} - R_n^{23}R_n^{21} + R_n^{23}R_n^{21}R_n^{34}R_n^{32} - R_n^{34}R_n^{21}T_n^{32}T_n^{23}}\right\}. \tag{59}$$

When $a_r \to 0$, i.e. when the thickness of layers shrinks to zero, Eq. (59) reduces to the transmission coefficient T_n^{41} for a homogeneous sphere of permittivity ε_4, as can be verified by inserting for the reflection and transmisssion coefficients. Notice that accomplishing the above approximation also implies restrictions on the permittivities ε_2 and ε_3.

By further algebra, Eq. (59) can be written explicitly in partial fractions

$$B_n^1 \approx T_n^{41}B_n^4 - a_r \times\left[n\eta_1 + \eta_2 + \frac{\eta_3}{n + \frac{\varepsilon_1}{\varepsilon_1+\varepsilon_4}} + \frac{\eta_4}{\left(n + \frac{\varepsilon_1}{\varepsilon_1+\varepsilon_4}\right)^2}\right]B_n^4, \tag{60}$$

where

$$\eta_1 = 2\varepsilon_4\frac{(\varepsilon_3-\varepsilon_2)(\varepsilon_1\varepsilon_3-\varepsilon_2\varepsilon_4) + (\varepsilon_3-\varepsilon_4)(\varepsilon_2-\varepsilon_1)(\varepsilon_2+\varepsilon_3)}{\varepsilon_2\varepsilon_3(\varepsilon_1+\varepsilon_4)^2} \tag{61}$$

$$\eta_2 = \frac{\varepsilon_4}{\varepsilon_2\varepsilon_3(\varepsilon_2+\varepsilon_3)(\varepsilon_1+\varepsilon_4)^3} \times\Big\{(\varepsilon_1+\varepsilon_4)\left[(\varepsilon_1^2-\varepsilon_3^2)(\varepsilon_1\varepsilon_4 - 2\varepsilon_1\varepsilon_3 + \varepsilon_2\varepsilon_3\right) + 2(\varepsilon_2-\varepsilon_1)(\varepsilon_3-\varepsilon_4)(\varepsilon_2+\varepsilon_3)^2 + 2\varepsilon_2(\varepsilon_3-\varepsilon_2)(\varepsilon_1\varepsilon_3-\varepsilon_2\varepsilon_4)\Big] + 2\Big[(\varepsilon_3-\varepsilon_2)(\varepsilon_1\varepsilon_3-\varepsilon_2\varepsilon_4) + (\varepsilon_2-\varepsilon_1)(\varepsilon_2+\varepsilon_3)(\varepsilon_3-\varepsilon_4)\Big]\left(\varepsilon_3\varepsilon_4 - \varepsilon_1(2\varepsilon_2+\varepsilon_3)\right)\Big\} \tag{62}$$

$$\eta_3 = \frac{\varepsilon_4}{\varepsilon_2\varepsilon_3(\varepsilon_2+\varepsilon_3)(\varepsilon_1+\varepsilon_4)^2}\Big\{2\Big[(\varepsilon_3-\varepsilon_2)(\varepsilon_1\varepsilon_3-\varepsilon_2\varepsilon_4) + (\varepsilon_2-\varepsilon_1)(\varepsilon_2+\varepsilon_3)(\varepsilon_3-\varepsilon_4)\Big] \times\frac{\left(\varepsilon_1(\varepsilon_2+\varepsilon_3)\left((\varepsilon_2+\varepsilon_3)(2\varepsilon_1-\varepsilon_4) + (\varepsilon_1+\varepsilon_4)(\varepsilon_2-\varepsilon_3)\right) - \varepsilon_2\varepsilon_3(\varepsilon_1+\varepsilon_4)^2\right)}{(\varepsilon_2+\varepsilon_3)(\varepsilon_1+\varepsilon_4)^2} + \frac{(\varepsilon_3\varepsilon_4 - 2\varepsilon_1\varepsilon_2 - \varepsilon_1\varepsilon_3)}{(\varepsilon_2+\varepsilon_3)(\varepsilon_1+\varepsilon_4)}\left((\varepsilon_2^2-\varepsilon_3^2)(\varepsilon_1\varepsilon_4 - 2\varepsilon_1\varepsilon_3 + \varepsilon_2\varepsilon_3) + 2(\varepsilon_2-\varepsilon_1)(\varepsilon_3-\varepsilon_4)(\varepsilon_2+\varepsilon_3)^2 + 2\varepsilon_2(\varepsilon_3-\varepsilon_2)(\varepsilon_1\varepsilon_3-\varepsilon_2\varepsilon_4)\right) + (\varepsilon_3-\varepsilon_4)(\varepsilon_3-\varepsilon_2)\varepsilon_1\varepsilon_2 + (\varepsilon_2-\varepsilon_1)\varepsilon_2\varepsilon_3(\varepsilon_2+\varepsilon_3-2\varepsilon_4)\Big\} \tag{63}$$

$$\eta_4 = \frac{\varepsilon_4\varepsilon_1}{\varepsilon_2\varepsilon_3(\varepsilon_2+\varepsilon_3)(\varepsilon_1+\varepsilon_4)^3} \times\Big\{2\Big[(\varepsilon_2-\varepsilon_3)(\varepsilon_1\varepsilon_3-\varepsilon_2\varepsilon_4) - (\varepsilon_2-\varepsilon_1)(\varepsilon_2+\varepsilon_3)(\varepsilon_3-\varepsilon_4)\Big] \times\frac{\left(\varepsilon_1\varepsilon_2(\varepsilon_1\varepsilon_2-\varepsilon_3\varepsilon_4) - \varepsilon_1\varepsilon_3\varepsilon_4(\varepsilon_2+\varepsilon_3) - \varepsilon_2\varepsilon_3\varepsilon_4(\varepsilon_1+\varepsilon_4)\right)}{(\varepsilon_2+\varepsilon_3)(\varepsilon_1+\varepsilon_4)^2} + \frac{(\varepsilon_2\varepsilon_1-\varepsilon_3\varepsilon_4)}{(\varepsilon_2+\varepsilon_3)(\varepsilon_1+\varepsilon_4)} \times\left((\varepsilon_2^2-\varepsilon_3^2)(\varepsilon_1\varepsilon_4 - 2\varepsilon_1\varepsilon_3 + \varepsilon_2\varepsilon_3) + 2(\varepsilon_2-\varepsilon_1)(\varepsilon_3-\varepsilon_4)(\varepsilon_2+\varepsilon_3)^2 + 2\varepsilon_2(\varepsilon_3-\varepsilon_2)(\varepsilon_1\varepsilon_3-\varepsilon_2\varepsilon_4)\right) - (\varepsilon_3-\varepsilon_4)(\varepsilon_3-\varepsilon_2)\varepsilon_1\varepsilon_2 - (\varepsilon_2-\varepsilon_1)\varepsilon_2\varepsilon_3(\varepsilon_2+\varepsilon_3-2\varepsilon_4)\Big\}. \tag{64}$$

Checking the result by letting $\varepsilon_3 = \varepsilon_4$ or $\varepsilon_1 = \varepsilon_2$, all coefficients will simplify to the respective coefficients (42) - (45) of the corresponding two-interface problem. On the other hand, with $\varepsilon_2 = \varepsilon_3$, the relative thickness of the layer of the sphere becomes $2a_r$, whence we obtain from the above formulae two times the value given by Eqs. (42) - (45). Furthermore, it is interesting to note the symmetry in the sense that when $\varepsilon_1 = \varepsilon_3$ and $\varepsilon_2 = \varepsilon_4$, all coefficients are equal to zero and, consequently, the layers have no effect on the image or on the field. This occurs only for the thin-layer sphere.

At this stage, the image source corresponding to Eq. (60) can be written as the image due to the homogeneous sphere (coefficient T_n^{41}) plus the perturbational part with a dipole, point charge, and line sources between $z = 0$ and $z = d$:

$$\varrho_i(z) \approx \frac{2\varepsilon_1}{\varepsilon_4 + \varepsilon_1} q\delta(z-d) + \frac{\varepsilon_1(\varepsilon_4 - \varepsilon_1)}{(\varepsilon_4 + \varepsilon_1)^2} \frac{q}{d} \left(\frac{z}{d}\right)^{-\varepsilon_4/(\varepsilon_2+\varepsilon_1)} \prod(0, z, d) - a_r q \frac{\varepsilon_1}{\varepsilon_4} \left[\eta_1 \delta'(d-z) + \eta_2 \delta(z-d) + \frac{\prod(0, z, d)}{d} \left(\frac{z}{d}\right)^{-\varepsilon_4/(\varepsilon_4+\varepsilon_1)} \left(\eta_3 + \eta_4 \ln\left(\frac{d}{z}\right)\right)\right]. \quad (65)$$

Evidently, when $a_r = 0$ the layers do not affect the image and, generally, the above image expression is the better thinner are the layers. Note also the resemblance with Eq. (41).

There also exist other possibilities to find approximate images from Eq. (57). For example, we may require that the outermost layer is very thick and the other layer is very thin, or vice versa, or assume that both layers are very thick, i.e., $a_3 \ll a_2 \ll a_1$. In the latter case the approximation for the image source may be constructed from the term $T_{43}T_{32}T_{21}$ of (57) in a similar manner as for two-interface sphere. It appears that adding more layers makes the analytical expressions for B_n^1 grow so that some restrictions concerning the thicknesses and/or permittivities of the layers will be necessary.

3
Point-source approximations

To compute potentials from the image source without integration the image charge density function must be approximated with point sources. These can be either isolated point charges on the image line or multipoles at a suitable expansion point. The isolated-point-charge approximation is performed by dividing the image line into segments and by replacing the original image charge distribution by a point charge at the center of gravity of the distribution on each segment. Below, we will compute the center of a gravity for the whole image line in the case of a two-layer sphere. If a multipole source is used, the expansion point should be chosen so that the number of terms is reduced to a minimum.

The general multipole source of amplitude M_p at the point $z = z_0$ satisfies

$$M_p = \int_0^{a_1} \varrho_i(z)\,(z - z_0)^p \, dz. \quad (66)$$

For $p = 0$, Eq. (66) gives the integral of the image source, which, provided that the function $\varrho_i(z)$ is exact, gives the total charge q.

Let us, for example, find the image multipoles corresponding to Eq. (41). By requiring the first moment of (66) to be zero ($M_1 = 0$), the location of the multipoles becomes

$$z_0 = d \frac{3\varepsilon_1}{2\varepsilon_1 + \varepsilon_3} \left[1 - 2a_r \frac{(\varepsilon_2 - \varepsilon_1)(\varepsilon_3 - \varepsilon_2)}{\varepsilon_2(2\varepsilon_1 + \varepsilon_3)}\right]. \quad (67)$$

This expansion point corresponds to the center of gravity of the image charge. If the line image is approximated by a single point charge, this should be placed at $z = z_0$. The position is seen to shift from $z = d$ towards the origin for $\varepsilon_3 > \varepsilon_1$ and outwards in the opposite case. Expanding the polynomials in (66) and evaluating the integrals analytically, we get

$$M_n = qd^p \left[\frac{2\varepsilon_1}{\varepsilon_1 + \varepsilon_3} + \frac{\varepsilon_1(\varepsilon_3 - \varepsilon_1)}{(\varepsilon_1 + \varepsilon_3)\left((p+1)\,\varepsilon_1 + p\varepsilon_3\right)}\right] - a_r q d^p \frac{\varepsilon_1}{\varepsilon_3} \left[p\xi_1 + \xi_2 + \xi_3 \left(\frac{\varepsilon_1 + \varepsilon_3}{(p+1)\,\varepsilon_1 + p\varepsilon_3}\right) + \xi_4 \left(\frac{\varepsilon_1 + \varepsilon_3}{(p+1)\,\varepsilon_1 + p\varepsilon_3}\right)^2\right]. \quad (68)$$

It turns out that $M_n \to 0$ faster for smaller values of d than for larger ones, which means that the calculation of potential is slower for eccentric sources. Notice that if the expansion point is chosen to be at the origin, we will actually retrieve the original multipole solution for the problem.

4
Conclusion

We have developed an electrostatic image theory for the layered sphere containing a point source. Static reflection and transmission coefficients were used when handling complicated expressions for the potentials. Our emphasis was on developing analytical image expressions and finding methods to allow calculation of potentials from these sources. Because the exact image expression for the two-interface sphere turned out to be complicated to handle, some special cases, including a thin layer and a low-contrast layer, were treated approximatively. All of the presented image expressions, especially the continuous parts, can be approximated by sets of point charges. The approximations might be utilized in the analysis of the electroencephalograms, in which the potential on the scalp caused by sources in the brain must be computed. Existing algorithms for doing this are generally quite slow; substitution of a source in a multishell sphere by a few point sources in a homogeneous medium would greatly improve the speed of forward computations, which would be useful in simulations and in the numerical solution of the inverse problem of EEG.

References

1. Lindell, I. V.: Electrostatic image theory for the dielectric sphere. Radio Sci. 27 (1992) 1–8
2. **Dassios, G.; Kleinman, R. E.:** On Kelvin inversion and low-frequency scattering. SIAM Review 31 (1989) 565–585
3. **Neumann, C.:** Hydrodynamische Untersuchungen: Leipzig, Teubner, 1883
4. **Sten, J. C.-E.; Lindell, I. V.:** Electrostatic image theory for the dielectric sphere with an internal source. Microwave and Optical Tech. Lett. 5 (1992) 579–602
5. **Lindell, I. V.; Ermutlu, M. E.; Sihvola, A. H.:** Electrostatic image theory for the layered dielectric sphere. IEE Proc. H 139 (1992) 186–192
6. **Lindell, I. V.; Sten, J. C.-E.; Nikoskinen, K. I.:** Electrostatic image solution for the interaction of two dielectric spheres. Radio Sci. 28 (1993) 319–329
7. **Lindell, I. V.; Sten, J. C.-E.; Kleinmann, R. E.:** Low-frequency image theory for the dielectric sphere. J. Electro. Waves Applic., Vol. 8, No. 3, 295–313, 1994
8. **Lindell, I. V.; Lehtola, E. A.:** Magnetostatic image theory for the permeable sphere. IEEE Trans. Magn. 28 (1992) 1930–1934
9. **Hosek, R. S.; Sances Jr., A.; Jodat, R. W.; Larson, S. J.:** The contributions of intracerebral currents to the EEG and evoked potentials. IEEE Trans. Biomed. Eng. BME-25 (1978) 405–413
10. **Cuffin, B. N.; Cohen, D.:** Comparison of the magnetoencephalogram and electroencephalogram. Electroenceph. Clin Neurophysiol. 47 (1979) 132–146
11. **Ary, J. P.; Klein, S. A.,; Fender, D. H.:** Location of sources of evoked scalp potentials: Corrections for skull and scalp thicknesses. IEEE Trans. Biomed. Eng. BME-28 (1981) 447–452
12. **de Munck, J. C.; van Dijk, B. V.; Spekreijse, H.:** An analytic method to determine the effect of source modeling errors on the apparent location and direction of biological sources. J. Appl. Phys. 63 (1988) 944–956
13. **Uzunoglu, N. K.; Ventouras, E.; Papageorgiou, C.; Rabavilas, A.; Stefanis, C.;** Inversion of simulated evoked potentials to charge distribution inside the human brain using an algebraic reconstruction technique. IEEE Trans. Med. Imaging 10 (1991) 479–484
14. **Stratton, J. A.:** Electromagnetic Theory: New York, McGraw-Hill, 1941
15. **Gradshteyn, I. S.; Ryzhik, I. M.:** Table of Integrals, Series, and Products: New York, Academic, Press, 1980